

**180-425 GHz LOW NOISE SIS WAVEGUIDE RECEIVERS
EMPLOYING TUNED Nb/AlO_x/Nb TUNNEL JUNCTIONS**

*J. W. Kooi¹, M. Chan¹, B. Bumble²,
H. G. LeDuc², P. L. Schaffer¹, and T.G. Phillips¹*

1- Caltech Submillimeter Observatory

Division of Physics, Mathematics and Astronomy

California Institute of Technology, Pasadena, California 91125

2- Center for Space Microelectronics Technology, Jet Propulsion Laboratory

Abstract

We report recent results on a 20% reduced height 270-425 GHz SIS waveguide receiver employing a $0.49\mu\text{m}^2$ Nb/AlO_x/Nb tunnel junction. A 50% operating bandwidth is achieved by using a RF compensated junction mounted in a two-tuner reduced height waveguide mixer block. The junction uses an "end-loaded" tuning stub with two quarter-wave transformer sections. We demonstrate that the receiver can be tuned to give 0-2 dB of conversion gain and 50-80% quantum efficiency over parts of its operating range. The measured instantaneous bandwidth of the receiver is ≈ 25 GHz which ensures virtually perfect double sideband mixer response. Best noise temperatures are typically obtained with a mixer conversion loss of 0.5 to 1.5 dB giving uncorrected receiver and mixer noise temperatures of 50K and 42K respectively at 300 and 400 GHz. The measured double sideband receiver noise temperature is less than 100K from 270 GHz to 425 GHz with a best value of 48K at 376 GHz, within a factor of five of the quantum limit. Preliminary tests of a similar junction design in a full height 230 GHz mixer block indicate large conversion gain and receiver noise temperatures below 50K DSB from 200-300 GHz. Best operation is again achieved with the mixer tuned for 0.5-1.5 dB conversion loss which at 258 GHz resulted in a receiver and mixer noise temperature of 34K and 27K respectively.

Introduction

A 20% reduced height waveguide superconductor-insulator-superconductor (SIS) heterodyne receiver with a center frequency of 345 GHz has been designed and installed at the Caltech Submillimeter Observatory (CSO) on Mauna Kea in Hawaii. The low noise results discussed here were achieved by employing a $0.49\mu\text{m}^2$ Nb/AlO_x/Nb tunnel junction with a lithographically produced "end-loaded" stub matching network to tune out the junction capacitance.

To improve the bandwidth and performance of the receiver over the suc-

successful Ellison design [2, 3], a 20% reduced waveguide mixer block with a tuned Nb/AlO_x/Nb tunnel junction was used. The mixer block incorporates magnetic field concentrators [4] and an octave wide bandwidth IF matching network [5]. A variety of inductive tuning stubs have been introduced [6, 7, 8, 9, 10, 11] to improve the junction match to the embedding impedance. In recent years quasi-optical techniques with lithographically produced matching structures have been successfully used to build sensitive submillimeter receivers [12, 13, 14]. A review of the conventional tuning circuits has been given by Zmuidzinas *et al.* [12]. The series tuned "end-loaded" stub as discussed by Büttgenbach *et al.* [13] has been used in the junction designs because it has several advantages over the conventional open and short circuit shunted stubs.

RF Matching Network

For an SIS tunnel junction the geometric capacitance of the two niobium films separated by a very thin insulator dielectric, ($\approx 12 \text{ \AA}$), is in parallel with the quantum of the tunnel barrier. For bias voltages on the first quasiparticle step the imaginary part of the junction's RF admittance is nearly zero, and the junction susceptance is dominated by the geometric capacitance, C_j . The RF conductance for a junction is described by Tucker's quantum theory.

$$G_j = \frac{e}{2\hbar\omega} \sum J_n^2(\alpha) \left[I_{dc} \left(V_o + \frac{(n+1)\hbar\omega}{e} \right) - I_{dc} \left(V_o + \frac{(n-1)\hbar\omega}{e} \right) \right] \quad (1)$$

In the low LO power limit where $\alpha \equiv eV_{io}/\hbar\omega < 1$, G_j is given by the slope of the line joining points on the pumped IV curve one photon step above and below the dc bias point [1, 15]. R_j (G_j^{-1}) ranges from $R_n/3$ in the lower part of the sub-millimeter band to R_n for frequencies $\geq 500 \text{ GHz}$. R_n is the above gap normal state resistance of the SIS tunnel junction. The admittance of the junction can thus be described as

$$Y_j = (G_j + i\omega C_j) \quad (2)$$

Where C_j is the junction capacitance, $\approx 65\text{-}85 \text{ fF}/\mu\text{m}^2$. The RF conductance varies slowly with frequency and for our design purposes is assumed to be constant. The coupling efficiency between two admittances has the form

$$\eta = \frac{4G_j G_p}{|Y_j + Y_p|^2} \quad (3)$$

Y_p is the admittance presented to the junction by the bow-tie antenna probe that is positioned in the center of the waveguide. This includes the reduced height waveguide impedance, $\approx 390 \text{ } \Omega$, which is transformed by means of a series

inductance (E-plane tuner) and shunt susceptance (backshort tuner). The probe admittance is a function of frequency but in the ideal case can be held constant by adjusting the E-plane and backshort tuners. For our design purpose we have taken Y_p to be constant. It is however possible to carefully model $Y_p(\omega)$ and use it to design tunerless mixers. This technique has not been attempted here, but could conceivably yield good results for imaging arrays. To obtain an optimum coupling efficiency it is required that $Y_p = Y_j^*$. The simplest way to achieve this condition is to tune out the junction susceptance with an open ended stub.

The admittance of a transmission line with a characteristic admittance $Y_o = Z_o^{-1}$ is given by

$$Y_s = Y_o \frac{Y_l + iY_o \tan(\beta l)}{Y_o + iY_l \tan(\beta l)} \quad (4)$$

β is the propagation constant $= 2\pi/\lambda$, Y_l the load impedance and βl the electrical length. For $Y_l=0$ (open circuit) the input susceptance becomes

$$B_s = iY_o \tan(\beta l) \quad (5)$$

The shunt susceptance of the open ended stub cancels the junction susceptance for $Y_o = \omega C_j$ and $l = 3/8 \lambda$ giving perfect coupling efficiency provided that the probe admittance is real and equals the RF conductance of the junction G_j . Similar results can be obtained with a shorted $1/8 \lambda$ transmission line or an ideal inductor. The latter requires a series capacitance to allow the junction to be dc biased and as such is not physically realizable at submillimeter wavelength's. For a $1/8 \lambda$ shorted stub we get

$$B_s = -iY_o \cot(\beta l) \quad (6)$$

The shorted stub provides a larger frequency range over which a match to the junction can be achieved. This can be observed by comparing the derivatives of (5) and (6). It can be shown that the open-circuited stub has a theoretical fractional bandwidth of $\approx 0.35 K^{-1}$ while the short-circuited stub has a bandwidth of $\approx 0.93 K^{-1}$, where $K \equiv \omega R_j C_j$. The main disadvantages of the open ended stub is the small bandwidth over which a good match can be achieved and the critical dependence of the match on the effective electrical length of the stub. The short-circuited stub has a nearly three times larger bandwidth than the open-circuit stub. Unfortunately the overall performance is still critically dependent on the actual stub length. In practice it is difficult to design a tuning stub that resonates at the design frequency. This is largely due to uncertainties in the manufacturing process and properties of niobium at 4K.

These problems can to some extent be overcome by the use of an "end-loaded" tuning circuit as discussed by several authors [13, 16]. The "end-loaded" stub puts a small section transmission line in series with the junction. This results

in the transformation of the complex junction admittance, Y_j to the real axis of the Smith Chart.

Consider a transmission line with a characteristic admittance $Y_o = \omega C_j$ and a load $Y_l = (G_j + i\omega C_j)$. Using (2) and (4) we calculate the electrical length of the "end-loaded" stub (βl_s) for which the imaginary part of Y_s equals zero.

$$\tan(\beta l_s) = \frac{Z_o^2}{2} \left(\sqrt{G_j^4 + 4Y_o^4} - G_j^2 \right) \quad (7)$$

Where Z_o is the characteristic impedance, Y_o^{-1} . We can simplify (7) for $G_j < Y_o$.

$$\tan(\beta l_s) \simeq 1 - \frac{1}{2K^2}, \quad K > 1.2 \quad (8)$$

Combining (8) and (4) we can solve for the real part of the transformed junction admittance.

$$G_s \simeq Y_o \left(\frac{K(2K^2 - 1)}{2K^4 - 2K^3\sqrt{K^2 - 1} - 1} \right), \quad l = l_s \quad (9)$$

For $\omega R_j C_j \gg 1$ equation (9) simplifies to

$$R_s \simeq \frac{R_j}{2K^2} \quad (10)$$

This is similar to an expression derived by Büttgenbach *et al.* [13] for $R_j \rightarrow R_n$. R_s is the transformed resistance of a junction connected to an "end-loaded" stub of electrical length βl_s (Fig. 5b). Expressing (9) in terms of the electrical length of the series transmission line we get

$$R_s \simeq R_j \cos(2\beta l_s) \quad (11)$$

As the frequency increases we see from (8) that the stub length l_s approaches $\pi/4$, which reduces R_s to very small values (11). This is a serious drawback of the "end-loaded" stub. For frequencies above 500 GHz it gets more and more difficult to transform R_s to match the probe impedance over a reasonable bandwidth (Fig. 1).

To transform R_s to Z_p^* , we used a two section equal-ripple Chebyshev transformer [17]. This type of transformer gives the maximum bandwidth while allowing a tolerable pass band ripple. If we define ρ_m as the maximum allowed voltage reflection coefficient of the passband ripple (Fig. 3), we can derive the impedances for the two quarter-wave sections that give the widest possible fractional bandwidth.

$$Z_1^2 = R_p \sqrt{R_s R_p} \sqrt{\frac{1 - \rho_m}{1 + \rho_m}} \quad (12)$$

$$Z_2^2 = R_s^2 \sqrt{\frac{R_p}{R_s}} \sqrt{\frac{1 + \rho_m}{1 - \rho_m}} \quad (13)$$

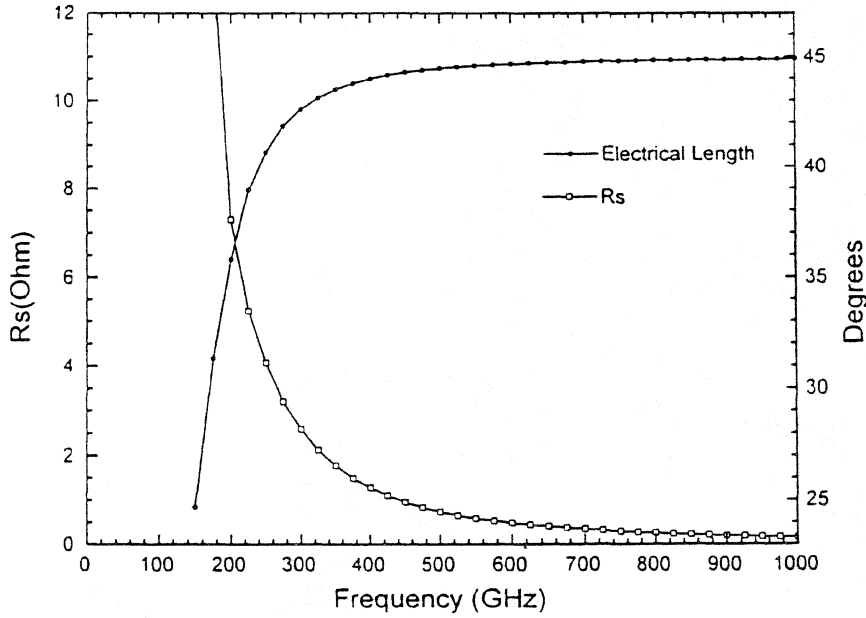


Fig. 1. The real part of the transformed junction impedance (9) and electrical length of the "end-loaded" stub (7) as a function of frequency. The junction's RF conductance is obtained from Tucker's theory. The calculations assume a $0.5 \mu\text{m}^2$, 8000 A/cm^2 tunnel junction with a geometric capacitance of 40 fF .

Z_1 is the high impedance section which connects to the probe and Z_2 is the low impedance section connected to the "end-loaded" stub (Fig. 5). Using (10) we can express Z_1 and Z_2 in terms of K and the RF resistance of the junction, R_j .

$$Z_1^2 \approx \frac{R_p}{K} \sqrt{\frac{R_j R_p}{2}} \sqrt{\frac{1 - \rho_m}{1 + \rho_m}}, \quad K \gg 1 \quad (14)$$

$$Z_2^2 \approx \frac{R_j}{4K^3} \sqrt{2R_j R_p} \sqrt{\frac{1 + \rho_m}{1 - \rho_m}}, \quad K \gg 1 \quad (15)$$

Equations (14) and (15) show that $Z_1 \propto K^{-0.5}$ and $Z_2 \propto K^{-1.5}$. For frequencies in the upper half of the submillimeter band Z_2 becomes very small

for junctions with current densities less than 10kA/cm^2 . In practice it is difficult to realize a very low impedance superconducting microstrip transmission line because its aspect ratio, (length/width), becomes rather small. Connecting the high impedance "end-loaded" stub to a low impedance transmission line results in a large discontinuity which increases the effective electrical length of the "end-loaded" stub. This is an especially serious effect at frequencies above 500 GHz considering that the center frequency of the RF matching network is critically dependent on the "end-loaded" stub's electrical length (Fig. 1). Figure 2 shows the calculated impedances of a two section quarter-wave transformer in the submillimeter band for a worst case in-band reflection coefficient, ρ_m , of -9 dB.

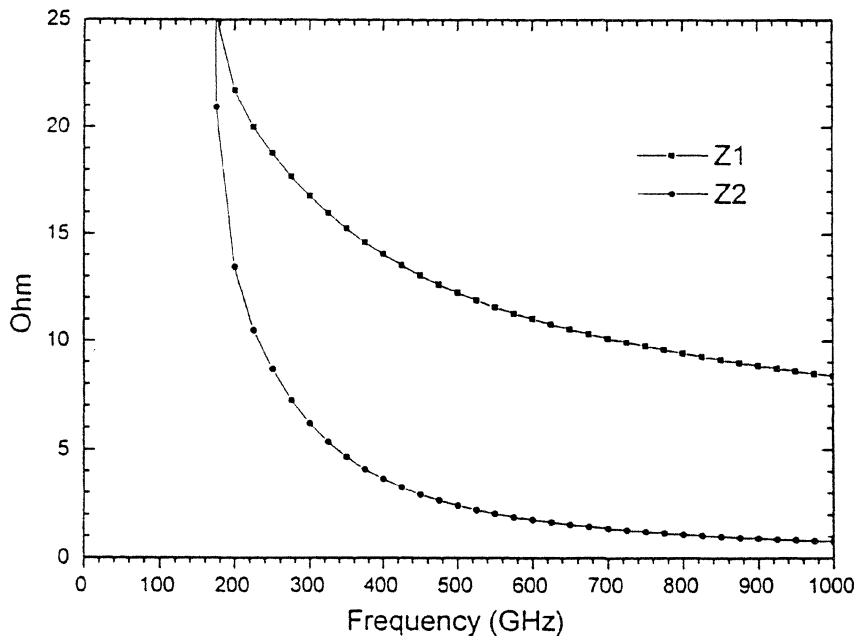


Fig. 2. Characteristic impedances of an equal-ripple two-section Chebyshev quarter-wave transformer needed to transform R_s (Fig. 1.) to a $40\ \Omega$ probe impedance. For frequencies exceeding 500 GHz $Z_2 < 2\ \Omega$, which makes implementation difficult.

Radially shorted inductive stubs [11] and two junction type tuning circuits as described by Zmuidzinas *et al.* [12] are good candidates for the upper half of the submillimeter band.

Junction Design

The waveguide of the 345 GHz mixer supports single, TE_{10} , mode operation from 222–444 GHz. The 270–420 GHz frequency band was chosen to be within these limits and to provide adequate overlap between the 230 and 492 GHz SIS receivers [4, 5]. These along with the newly installed 665 GHz receiver [18] provide complete coverage for the 180–730 GHz CSO submillimeter astronomy band. To achieve a good match over the desired 270–420 GHz frequency band it is imperative that a probe impedance, $Z_p(\omega)$, is selected that can easily be tuned to over the entire frequency range [19]. Räsänen *et al.* [20] have made scale model measurements on full and reduced-height waveguide embedding impedances. Their data indicates that the embedding impedance of a probe, with 45 degree lead shapes, at the center frequency of the mixer is slightly inductive and has a real part less than 50Ω . This result has recently been confirmed Honingh *et al.* [21]. For our "end-loaded" stub design we assumed the probe impedance equal to $40 + 10i \Omega$.

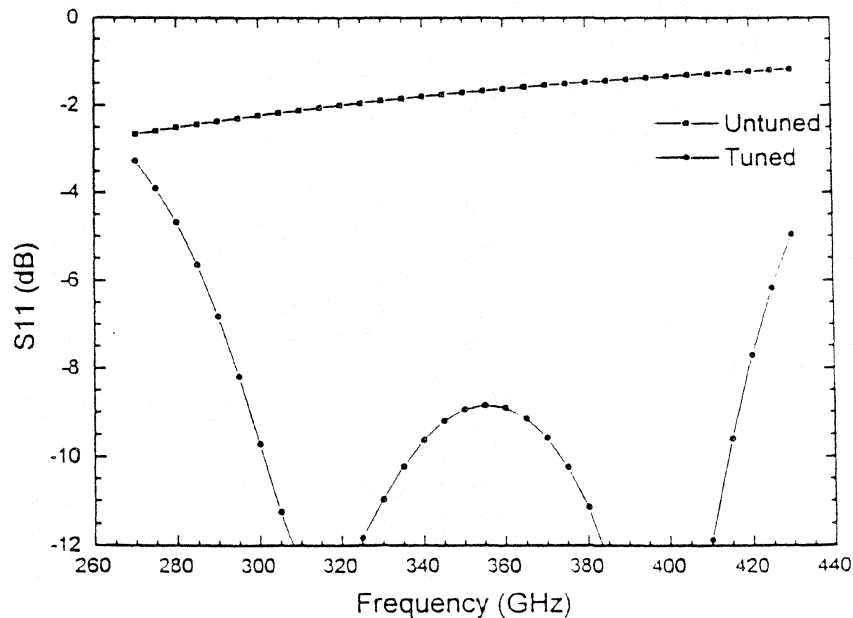


Fig. 3. Input reflection coefficient (dB) of a tuned and untuned 50Ω $0.49 \mu\text{m}^2$ Nb/ AlO_x /Nb tunnel junction. The designed inband reflection coefficient is -9 dB, which was a trade off between maximum RF bandwidth and optimum impedance match.

By adjusting the non-contacting tuners we keep $Z_p(\omega)$ approximately constant over the entire frequency range [16]. To keep the $\omega R_j C_j$ product (K) as small as possible, allow good coupling to an IF impedance of 160Ω [5], and maintain high quality junctions we decided to use 50Ω $0.49\mu\text{m}^2$ Nb/ AlO_x /Nb SIS tunnel junctions with current densities of ≈ 8000 A/cm². Using (1) the RF resistance of the pumped IV curve for small values of alpha is approximately $.67R_n$ at 345 GHz and $0.55R_n$ at 230 GHz.

In Fig. 4 we plot the junction impedance of an "end-loaded" stub tuned junction and untuned junction.

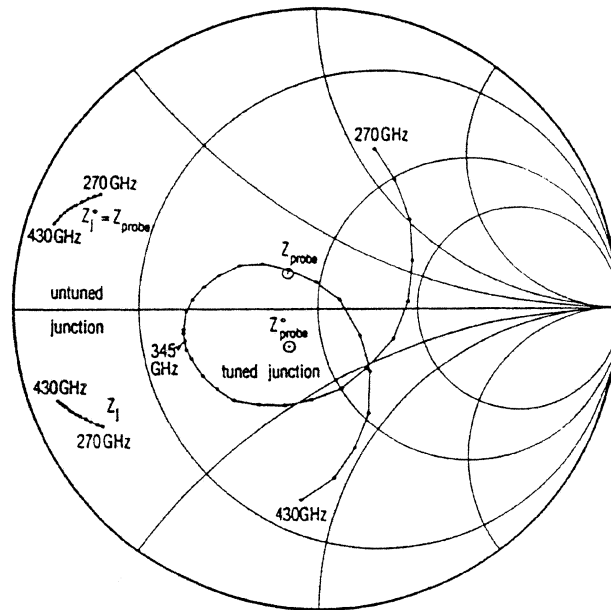


Fig. 4. Tuned and untuned junction impedance plot. The tuned junction is matched to Z_p . For untuned junctions very high quality (Q) tuners are needed to tune the probe impedance to Z_j^* .

The "end-loaded" stub length and transformer impedance sections Z_1 and Z_2 were initially calculated using a 40Ω probe impedance. We then ran Touchstone [22] to optimize the transformer for a probe impedance $Z_p = 40 + 10i \Omega$. The width's and length's of the optimized normal metal microstrip were used to calculate the characteristic impedance and electrical length of the individual sections using Linecalc [22].

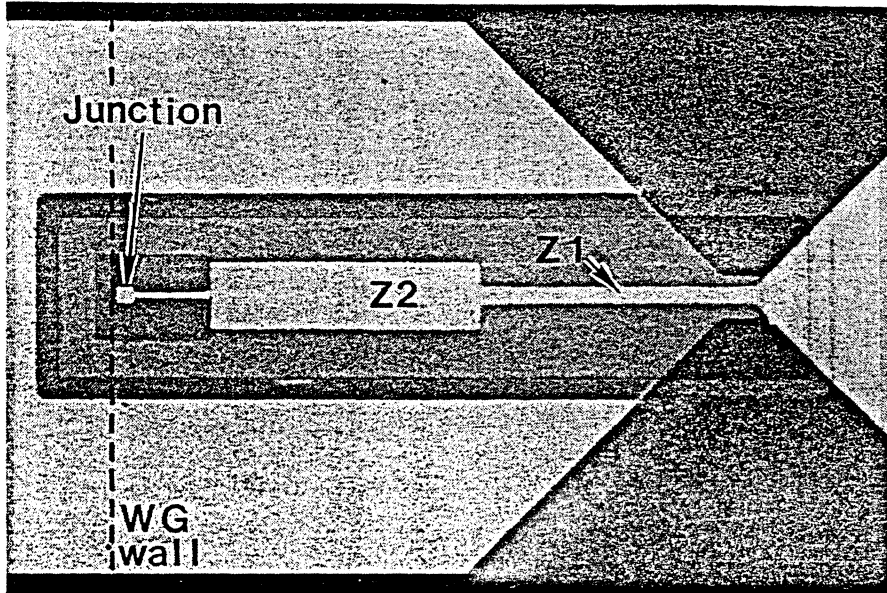


Fig. 5. (a) Physical layout of a 230/345 GHz tuned junction. The junction and "end-loaded" stub are fabricated on 150nm SiO while the two section transformer is fabricated on 450nm SiO. The junction is deposited inside a $5 \times 5 \mu\text{m}^2$ pad whose effect has been taken into account in the computer simulations. At 345 GHz the width and electrical length of the "end-loaded" stub are $2\mu\text{m}$ and 39.8 degrees respectively.

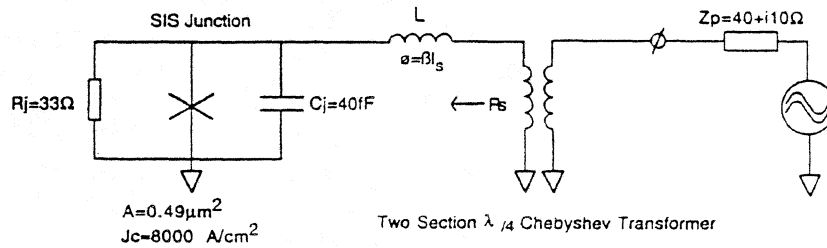


Fig. 5. (b) Electrical diagram of the RF matching network at 345 GHz. The probe impedance is defined as the impedance seen by the bowtie antenna placed in the center of the waveguide.

Using a program developed by Zmuidzinas *et al.* [23], which is based on work by Whitaker, Kautz, Hammerstad and Jensen, we proceeded to calculate the required superconducting microstrip width, length and effective dielectric constant of the different line sections. This procedure was iterative because the junction mask was layed out using integer length and width dimensions for different superconducting microstrip transmission line sections. The numerical results of the superconducting transmission line sections are summarized below.

Table 1

230 GHz and 345 GHz Tuned Junction Parameters.

	230 Theory	230 Optimized Results	345 Theory	345 Optimized Results
$Z_p^*(\Omega)$	$40 + 0i$	$40 - 10i$	$40 + 0i$	$40 - 10i$
ρ_m	0.2512	0.2445	0.3548	0.3631
$\beta l_s(^{\circ})$	38.3	40.2	43.2	39.8
$Y_o(\Omega^{-1})$	0.0578	0.0702	0.0867	0.0692
$R_s(\Omega)$	5.28	4.01	1.95	1.87
$Z_1(\Omega)$	20.86	16.41	15.62	13.64
$Z_2(\Omega)$	9.48	6.22	4.95	4.06

Nb/AlO_x/Nb Junction Fabrication

Fabrication of the Nb/AlO_x/Nb tunnel junction is accomplished using a standard trilayer deposition technique [24]. The trilayer is patterned on a 200 μm thick, 25mm diameter fused quartz substrate by a lift-off process employing image reversal of AZ5206 photoresist. Magnetron sputter deposition and room temperature oxide growth are done in-situ in an ultra-high vacuum system with a base pressure of 5×10^{-9} Torr. One side of the antenna/filter structure is formed by the trilayer with 160nm Nb base, 6nm Al, and a 90nm Nb counter-electrode. A junction mesa of $0.49 \mu\text{m}^2$ area is defined by direct write electron beam lithography in a 100nm thick PMMA stencil. Chromium is deposited through the PMMA stencil and serves as an etch mask over 500nm of polyimide. Contact regions of the trilayer are then protected with a photoresist stencil. The combined chromium+photoresist/polyimide structure is etched using an oxygen reactive ion etch (RIE) process step. Polyimide remaining defines an isolation window and junction mesa for subsequent Nb RIE. To achieve Nb etch directly

we utilize a gas mixture of 62% CCl_2F_2 + 31% CF_4 + 7% O_2 . Electrical isolation of the base electrode from the wire layer is provided by thermal evaporation of 150nm of SiO. Samples are rotated at a slight tilt angle during SiO deposition to assure both good isolation and self-aligned lift-off with the polyimide. After this lift-off step, another photoresist pattern is used to produce SiO thickness of 450nm on both transformer sections. The second half of the antenna/filter is formed by a blanket deposition of 300nm Nb capped with 30nm gold for contacts. Processing is completed by RIE etching and subsequent dicing of the wafer with a diamond saw [25]. Tunnel junctions with areas down to $0.25\mu\text{m}^2$ have been fabricated using this technique.

Receiver Description

Optics

The block diagram of the 345 GHz receiver is similar to that of the 665 GHz receiver [18]. The optics was designed to give a 14 dB edgetaper on the secondary mirror of the telescope. Local oscillator (LO) injection is accomplished with a 13 μm mylar beam splitter mounted at 45° to the LO path. The local oscillator's electric field is perpendicular to the plane of incidence and about 1.8% of the radiation couples into the cryostat, the remainder is absorbed by a sheet of Eccosorb. The vacuum window is made out of 19 μm HR500/2S material manufactured for food packaging by Hercules Inc. [26]. It has a dielectric constant of ≈ 2.6 and is a laminate of biaxially oriented polypropylene with 2.5 μm layers of polyvinylidene chloride on both sides. Laboratory experiments have shown that the material has adequate strength to function as a vacuum window for apertures diameters ≤ 25 mm. Experiments indicate that this Hercules material is considerably more opaque to He^4 than 25 μm mylar. The material is also expected to have a low permeability to water and atmospheric gasses. The infrared blocking filter on the 12K window consists of a half wavelength thick fluorogold disk. The mixer lens is made out of low density polyethelene, with an approximate dielectric constant of 2.41 at 4.2K ambient temperature. To better understand the nature of the optical losses we measured the transmission losses of selected materials. With the receiver tuned to 345 GHz we obtained the hot (293K) and cold (80K) IF power response with and without an optically thick 'lossy' slab of material inserted in the beam [18, 27]. The measured transmission losses for mylar and fluorogold at 345 GHz are shown in Table 2.

Table 2

345 GHz Measured Absorption Losses

Material	Dielectric Constant (ϵ')	α (np/mm)	$\tan(\delta)$
Fluorogold	2.56-2.64	.0266	4.5×10^{-3}
Mylar	3.0	.288	3.8×10^{-2}

The optics are designed to give a frequency independent illumination of the secondary (Goldsmith [28]). The low loss polyethylene lens is placed in the near field of the scaler feedhorn. Antenna pattern measurements give reasonably close agreement to the theoretically expected response.

345 GHz Mixer Block Construction

The 20% reduced waveguide mixer block is based on the full-height 230 GHz waveguide design by Ellison *et al.* [2] and uses magnetic field concentrators as discussed by Walker *et al.* [4]. The mixer block utilizes a double tuning structure and is composed of four sections. The front section constitutes the corrugated feedhorn with a beam waist of 1.44 mm. The second section holds the circular to rectangular waveguide transformer and E-plane tuner. Six quarter-waveguide wavelength transitions were used to transform the circular TE₁₁ mode to the reduced height TE₁₀ mode over the specified frequency range. The E-plane tuner is situated $1/2\lambda_g$ in front of the junction. The third section is the junction block with the built in IF matching network, while the last section holds the non-contacting rectangular backshort tuner. A 200 μm by 200 μm groove cut across the face of the waveguide and parallel to the E-field holds the junction. The fused quartz substrate dimensions are 175 μm in width and 100 μm in height. Care has been taken to center the bowtie antenna in the waveguide. Silver paint has been used to make contact with both ground and IF side of the RF choke. The IF side of the junction contacts a 25 μm Au wire which is soldered to a 1-2 GHz wide IF matching network situated in the junction block [4, 5]. The matching network is designed to transform a 160 Ohm IF impedance to 50 Ohms and to provide a short to out of band signals up to \approx 22 GHz. The latter is needed to avoid saturating the junction with unwanted out of band signals. The output of the mixer block is directly connected to a 1-2 GHz 5K balanced HEMT amplifier, which is based on work by Padin *et al.* [29]. Any impedance mismatch between the matching network and low noise amplifier is absorbed by the amplifier's input Lange coupler. The RF choke structure is a 4 section Chebyshev bandpass filter designed to give maximum rejection ($S_{11} \leq -23$ dB) at 345 GHz. Rectangular non-contacting tuners are

used in the mixer block for both the backshort and E-plane tuners as described by Brewer and Räsänen [30]. Both tuners have three low and high impedance sections. Circular non-contacting tuners [18, 31] give higher VSWR ratios (more ideal) and are excellent candidates for use with uncompensated junctions.

Results and Discussion

The 376 GHz pumped/unpumped I-V curves and hot(295K)/cold (80K) total power response are shown in Figure 6. The Josephson oscillations were carefully suppressed by adjusting the magnetic field.

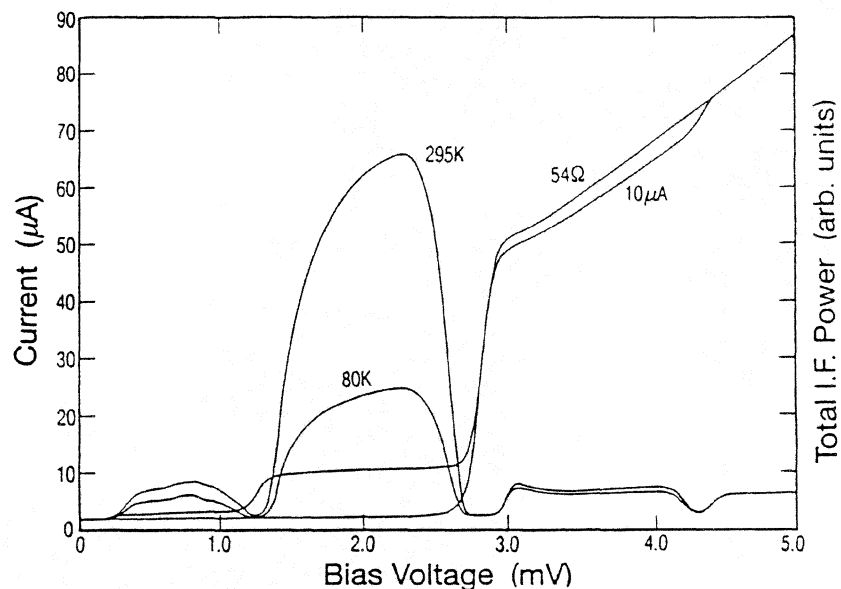


Fig. 6. I-V/Total power response. The optimum receiver noise temperature at 376 GHz was 48K DSB with an uncorrected mixer noise temperature of ≈ 40 K and 0.5dB of mixer conversion loss. The junction has a sub-gap leakage of $1.25 \mu\text{A}$.

The pumped I-V curve is nearly flat below the gap which is an indication that the junction is well matched to the probe impedance. With a $10\text{k}\Omega$ current bias circuit it was impossible to hold the junction voltage stable for very large or negative sub-gap impedances. To provide a stable voltage bias to the junction

we put a 100Ω resistor in parallel with the junction and a 20Ω current sense resistor in series with the junction [32, 33].

Best receiver noise temperatures were typically obtained with the receiver tuned for a mixer conversion loss of 0.5-1.5 dB. In this case the slope of the sub-gap pumped I-V curve is still slightly positive providing some reasonable IF impedance to the matching network. For large conversion gains the slope of the pumped sub-gap I-V curve is negative giving reflection gain. With the Josephson effect suppressed reflection gain can be readily observed from instabilities in the IF power response. Pumped I-V curves with negative slopes were easily detected with the $10k\Omega$ current bias by monitoring the voltage across the junction on an oscilloscope. By de-tuning the mixer backshort we could stabilize the junction bias which nearly always resulted in a slight conversion loss and optimum receiver sensitivity. The voltage bias circuit solves bias instability problems but does not provide a convenient feedback to detect possible mixer conversion gain. As the sub-gap IF impedance approaches infinity, ideally a transresistance amplifier is needed since the junction now acts as a current source. With the existing IF matching scheme, a cooled isolator or balanced IF amplifier is needed to absorb the large reflections between the junction and low noise amplifier.

For SIS mixers operating with a mixer conversion loss > 3 dB it is common to tune for maximum IF power or pumped junction current. Tuning for maximum IF power under these conditions nearly always gives the lowest mixer conversion loss because the IF mismatch is very small and the receiver output noise power is almost completely determined by the mixer conversion loss. The conversion loss was derived from the shot noise method [34], and has been corrected for the IF mismatch between the junction and low noise amplifier. With conversion gains > -2 dB the IF junction impedance is $\gg R_n$, which increases the IF mismatch and limits the sensitivity of the receiver. The optimum trade-off between mixer conversion gain and IF coupling efficiency is typically found by first tuning the receiver for maximum IF power (or pumped SIS current) and then optimizing the Y-factor by adjusting the backshort tuner. The receiver response of Fig. 6 was optimized for lowest noise temperature (i.e. largest Y-factor) instead of maximum IF noise power.

To confirm the calculated mixer noise temperature we used a technique described by Blundell *et al.* [35, 36]. By plotting the total IF power as a function of input load temperature for different values of LO drive level we obtained a mixer noise temperature of $38 \pm 2K$, in good agreement with the shot noise result (Fig. 6). At 376 GHz the calculated optics loss contributes $\approx 26K$ to the mixer noise temperature. By taking into account the increase of mixer noise temperature (3.8K) over the quantum limit due to the sub-gap leakage current [37], we calculate a SSB mixer response of $22K \pm 3K$ (≈ 1.2 times the quantum noise limit).

Fig. 7 depicts the uncorrected mixer, receiver noise temperatures and conversion gain at 376 GHz as a function of bias voltage with the receiver tuned for maximum IF power response. Although not clear from the graph the total power did have some instability. Note that even though the mixer exhibits conversion gain the receiver noise temperature does not decrease accordingly. The receiver sensitivity is limited to $\approx 50\text{K DSB}$ by the IF coupling efficiency and front-end loss generated noise ($\approx 26\text{K}$). It is possible to trade IF coupling efficiency for mixer conversion gain in certain parts of the frequency band. This has little or no effect on the receiver sensitivity but does degrade the stability of the receiver.

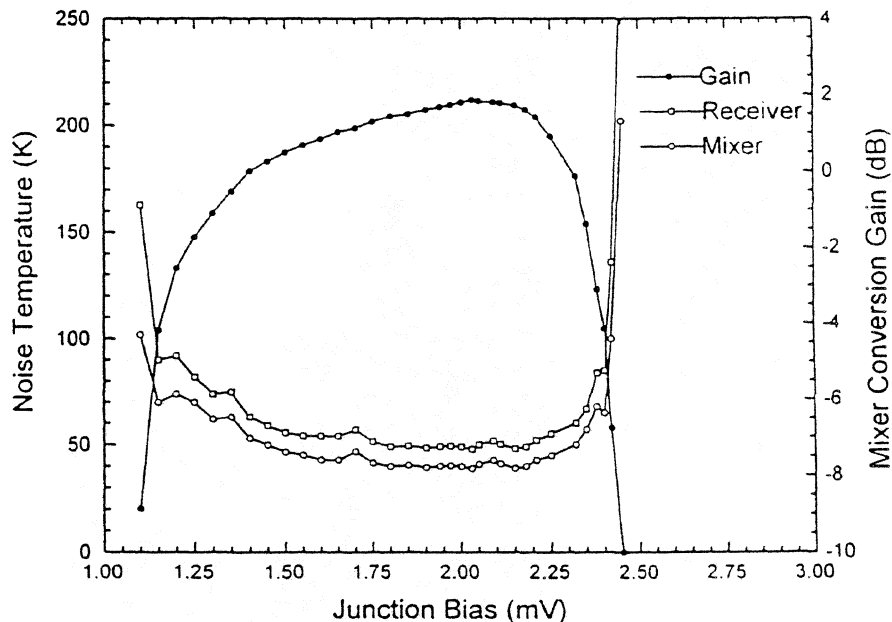


Fig. 7. Noise temperatures of the receiver and mixer, and conversion gain as a function of bias voltage at 376 GHz. The corrected SSB mixer noise temperature is $\approx 22\text{K}$ (80% quantum efficiency). The optimum bias voltage is between 2.0 and 2.2 mV which is similar to the 230, 492, and 665 GHz Nb/ AlO_x /Nb SIS quasi-particle receivers currently in operation at the CSO.

Stable operation and optimum receiver sensitivity is typically obtained with a conversion gain of $-1 \pm 0.5\text{ dB}$, (Fig. 6).

The instantaneous bandwidth for the "end-loaded" stub tuned junctions is ≈ 25 GHz, which ensures true double sideband mixer performance.

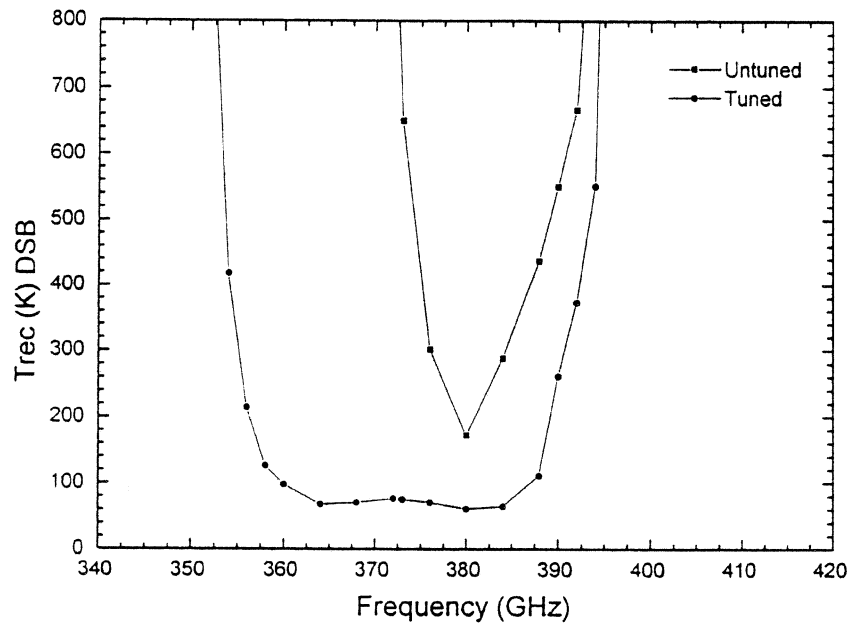


Fig. 8. Instantaneous bandwidth of both a tuned and untuned junction with the receiver centered at 380 GHz. The asymmetry of the tuned response is determined by the corner frequency of the RF matching network, ≈ 390 GHz. A similar result is seen at 300 GHz giving an effective tuned bandwidth of approximately 90 GHz (26%).

The measured DSB receiver noise temperature was less than 100K between 275-425 GHz. Fig. 9 depicts the frequency response of the receiver overlaid by the atmospheric transmission (1mm H₂O) on Mauna Kea, Hawaii. The receiver covers several atmospheric bands and fills the gap between the 230- and 492 GHz SIS receivers. The double tuned response of the equal-ripple transformer is evident from the receiver's frequency response (Fig. 3.). At 345 GHz the mixer conversion loss is ≈ 3 dB, which allows tuning for the maximum noise power as discussed in the text. Of course it is possible to trade bandwidth for sensitivity and to design an RF matching network which gives a better match in the center of the band.

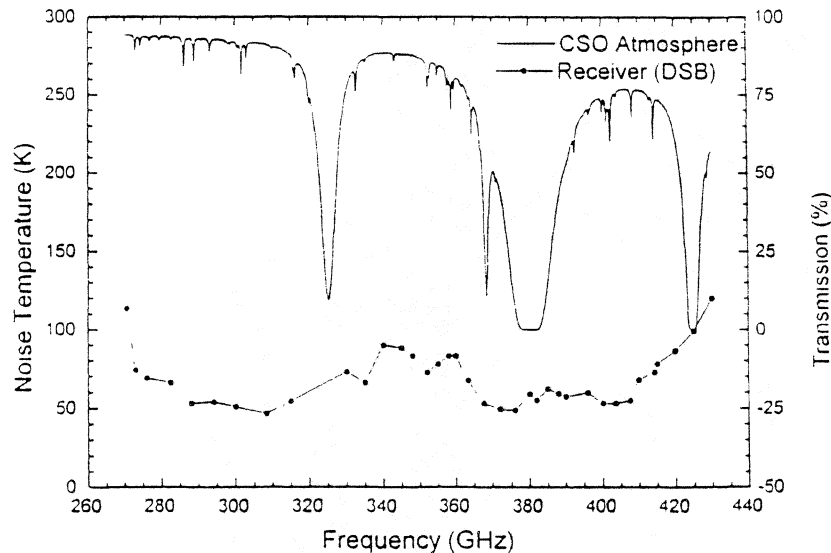


Fig. 9. Frequency response of the 345 GHz receiver from 270-430 GHz.

230 GHz Receiver Results

The 230 GHz "end-loaded" stub tuned junction was tested in a full height waveguide mixer block [2, 5]. Preliminary measured receiver noise temperatures vary from 30K-50K DSB across the 200-300 GHz band. Magnetic field concentrators to suppress Josephson oscillations were not incorporated in the mixer block [4]. For frequencies above 260 GHz we noticed small fluctuations in the total power response, which is attributed to our inability to suppress the Josephson effect. Conversion gain was encountered over much of the 200-300 GHz range, however best results were again obtained with the receiver tuned for 0.5-1.5 dB mixer conversion loss. The pumped/unpumped I-V curves and the hot(295K)/cold(80K) total power response are shown in Fig. 10.

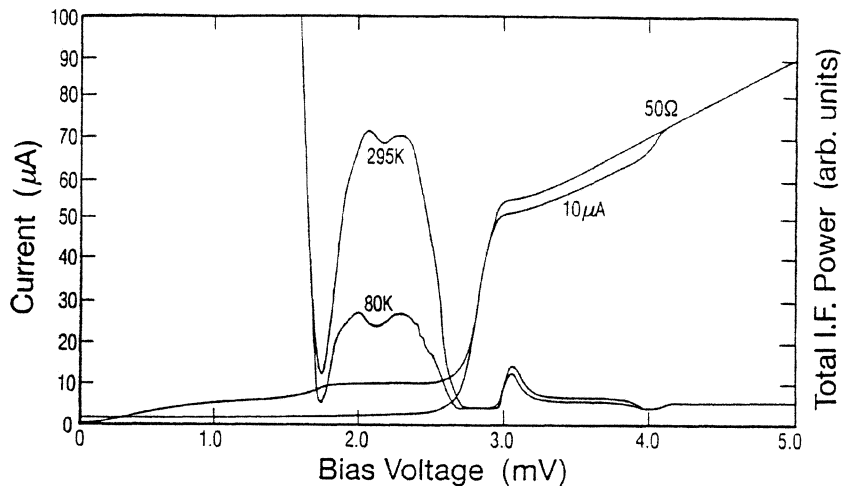


Fig. 10. Pumped and unpumped total power and I-V curves at 258 GHz. The measured receiver noise temperature at 2.05 mV bias was 34K DSB, ≈ 5.5 times the quantum noise limit. The mixer has an uncorrected noise temperature of $27\text{K} \pm 2\text{K}$, 0.5 dB of conversion loss and $\approx 70\%$ quantum efficiency. The junction has a current density of $\approx 8000 \text{ A/cm}^2$ and a sub-gap leakage of $1.25 \mu\text{A}$.

Conclusion

A SIS heterodyne quasi-particle mixer has been developed for the 270-430 GHz submillimeter band. The mixer employs a tuned $0.49 \mu\text{m}^2$ Nb/ AlO_x /Nb tunnel junction mounted in a 20% reduced height waveguide block. The RF matching network consists of an "end-loaded" stub with a two section equal-ripple transformer, which in combination with a two-tuner reduced height waveguide mixer block provides for 50% overall and 7% instantaneous bandwidth. The receiver has a double sideband noise temperature of $< 100\text{K}$ from 270-425 GHz and has been successfully installed at the Caltech Submillimeter Observatory in Hawaii. 1-3 dB of conversion gain and 50-80% quantum efficiency has been demonstrated over parts of the 180-430 GHz frequency band. As the junction capacitance is tuned out the junction behaves like a current source and has a receiver noise temperature that is limited by the front-end loss and the IF coupling

efficiency. Under the condition of near unity mixer conversion gain higher current density junctions should ideally be used to improve the IF match and retain the same RF bandwidth. The receivers can be tuned for either a slight conversion loss and good IF match, or conversion gain and poor IF match! The latter condition should be avoided. Best receiver sensitivity and stability is typically achieved with the mixer tuned for 0.5-1.5 dB conversion loss, which minimizes the IF noise contribution. For frequencies above 500 GHz the real part of the transformed junction impedance and the physical length of the transmission lines become very small. This reduces the bandwidth over which a good RF match can be achieved and at the same time dictates a very low impedance value for the second transformer section, with L/W ratio's near unity. In this case the junction becomes part of the "end-loaded" stub which introduces serious modeling and fabrication problems. For frequencies exceeding 500 GHz radially shorted tuning stubs and two junction matching techniques as described by Zmuidzinis *et al.* are good candidates for tuned junction designs. The "end-loaded" stub is a promising technology for the lower half of the submillimeter band. It enables development of tuned waveguide mixers with high quantum efficiency as well as fix-tuned receivers for use in imaging arrays.

Acknowledgments

We wish to thank Jonas Zmuidzinis, Thomas Büttgenbach, Chris Walker, Rob Schoelkopf, Todd Groesbeck, George Ugras, Dominic Benford, Dave Woody, Mei Bin, John Cortese and Tony Kerr for helpful discussions and John Carlstrom for supplying the 100-143 GHz wideband Gunn oscillators which were a tremendous aid in measuring the frequency response of the mixers. Work at Caltech is supported in part by NSF grant[#] AST-9015755 and NASA grant[#] NAGW-107.

References

- [1] J.R. Tucker and M.J. Feldman, "Quantum Detection at Millimeter Wavelength," *Rev. Mod. Phys.* 57, 1055-1113, 1985
- [2] B.N. Ellison and R.E. Miller, "A Low Noise 230 GHz SIS Receiver," *Int. J. IR and MM Waves*, Vol 8, 609-625, 1987
- [3] B.N. Ellison, P.L. Schaffer, W. Schaal, D. Vail, and R.E. Miller, "A 345GHz SIS Receiver for Radio Astronomy," *Int. J. IR and MM Waves*, Vol 10, No. 8, 1989
- [4] C.K. Walker, J.W. Kooi, M. Chan, H.G. Leduc, P.L. Schaffer, J.E. Carlstrom, and T.G. Phillips, "A Low-noise 492 GHz SIS waveguide receiver," *Int. J. IR and MM Waves*, Vol. 13, pp. 785-798, June 1992.
- [5] J.W. Kooi, M. Chan, T.G. Phillips, B. Bumble, and H.G. Leduc, "A low noise 230 GHz heterodyne receiver employing $0.25 \mu\text{m}^2$ area Nb/AlO_x/Nb tunnel junctions," *IEEE trans. Microwaves Theory and Techniques*, Vol. 40, pp. 812-815, May 1992.
- [6] L.R. D'addario, "An SIS Mixer for 90-120 GHz with Gain and Wide bandwidth," *Int. J. IR and MM Waves*, Vol 5, No. 11, pp. 1419-1433, 1984.
- [7] A.V. Räisänen, W.R. McGrath, P.L. Richards, and F.L. Lloyd, "Broad-band RF match to a Millimeter-Wave SIS Quasi-Particle Mixer," *IEEE Trans. Microwave Theory and Techniques*, Vol. MTT-33, No. 12, pp. 1495-1499, 1985.
- [8] A. R. Kerr, S.K. Pan, M.J. Feldman, "Integrated Tuning for SIS Mixers," *Int. J. IR and MM Waves*, Vol 9, No. 2, pp. 203-212, 1988.
- [9] C.E. Honingh, G. de Lange, M.M.T.M. Dierichs, H.H. Schaeffer, Th. de Graauw, and T.M. Klapwijk, "Performance of a Two-Junction Array SIS-Mixer Operating Around 345 GHz," *IEEE Trans. Microwave Theory and Techniques*, Vol. MTT-41, No. 4, pp. 616-623, 1993.
- [10] G. de Lange, C.E. Honingh, M.M.T.M. Dierichs, H.H.A. Schaeffer, H. Kuipers, R.A. Panhuyzen, T.M. Klapwijk, H. van de Stadt, M.W.M. de Graauw, and E. Armandillo, "Quantum limited responsivity of a Nb/Al₂O₃/Nb SIS waveguide mixer at 460 GHz", Proc. 4th Int'l Symp. Space THz Technology, Los Angeles, pp. 41-49, 1993
- [11] M. Salez, P. Febvre, W.R. McGrath, B. Bumble, H.G. LeDuc, "An SIS Waveguide Heterodyne Receiver for 600 GHz - 635 GHz," *Int. J. IR and MM Waves*, Vol 15, No. 2, Feb. 1994.
- [12] J. Zmuidzinas, H.G. Leduc, J.A. Stern, and S.R. Cypher, "Two-junction tuning circuits for submillimeter SIS mixers," *IEEE accepted*.

- [13] T.H. Büttgenbach, H.G. LeDuc, P.D. Maker, T.G. Phillips, "A Fixed Tuned Broadband Matching Structure for SIS Receivers," *IEEE Trans. Applied Supercond.*, Vol. 2, No. 3, pp. 165-175, 1992.
- [14] K.F. Schuster, A.I. Harris, K.H. Gundlach, "A 691 GHz SIS Receiver for Radio Astronomy," *Int. J. IR and MM Waves*, Vol 14, No. 10, Oct. 1993.
- [15] E.C. Sutton, "A Superconducting Tunnel Junction Receiver for 230 GHz," *IEEE Trans. Microwave Theory and Techniques*, Vol. MTT-31, No. 7, pp. 589-592, 1983.
- [16] K. Jacobs, U. Kothaus, and B. Vowinkel, "Simulated Performance and Model Measurements of an SIS Waveguide Mixer using Integrated Tuning Structures," *Int. J. IR and MM Waves*, Vol 13, No. 1, pp. 15-26, 1992.
- [17] "Foundations for Microwave Engineering," McGraw-Hill Physical and Quantum Electronics Series. 1966.
- [18] J.W. Kooi, C.K. Walker, H.G. LeDuc, T.R. Hunter, D.J. Benford, and T.G. Phillips, "A Low Noise 665 GHz SIS Quasi-Particle Waveguide Receiver," submitted to *Int. J. IR and MM Waves*, December 1993.
- [19] T.H. Büttgenbach, T.D Groesbeck, and B.N. Ellison, "A Scale Mixer Model for SIS Waveguide Receivers," *Int. J. IR and MM Waves*, Vol 11, no 1, 1990.
- [20] A.V. Räisänen, W.R. McGrath, D.G. Crete, and P.L. Richards, "Scale Model Measurements of Embedding Impedances for SIS Waveguide Mixers," *Int. J. IR and MM Waves*, Vol 6, No. 12, pp. 1169-1189, 1985.
- [21] C.E. Honingh, "A Quantum Mixer at 350 GHz based on Superconducting-Insulator-Superconducting (SIS) Junctions," PhD Dissertation, Groningen, The Netherlands, June 1993.
- [22] HP/EESOF CAD, Westlake Village, Ca. 91362.
- [23] J. Zmuidzinas, and H.G. LeDuc, "Quasi-Optical Slot Antenna SIS Mixers," *IEEE Trans. Microwave Theory and Techniques*, Vol. MTT-40, No. 9, pp. 1797-1804, September 1992.
- [24] M. Gurivch, M.A. Washington, and H.A. Huggins, "High Quality Josephson Tunnel Junctions Utilizing Thin Aluminum Layers," *Appl. Phys. Lett.*, v.42, 472-474, 1983.
- [25] H.G. LeDuc, B. Bumble, S.R. Cypher, and J.A. Stern, *Second International Symposium on Space Terahertz technology*, Pasadena, Ca. Feb. 26-28 (1991).
- [26] A.R. Kerr, N.J. Bailey, D.E. Boyd and N. Horner, "A study of materials for a broadband millimeter-wave quasi-optical vacuum window," Electronics Division Internal Report No. 292, National Radio Astronomy Observatory, Charlottesville, VA 22903, August 1992.
- [27] J. W. Lamb, "Infrared filters for cryogenic receivers," Electronics Division Internal Report No. 290, National Radio Astronomy Observatory, Charlottesville, VA 22903, April 1992.

- [28] P.F. Goldsmith, "Quasi-Optical techniques at Millimeter and Submillimeter Wavelength," . *Infrared and Millimeter Waves*, Vol 6, pp. 277-343, 1982.
- [29] S. Padin, G. Ortiz, "A Cooled 1-2 GHz Balanced HEMT Amplifier," *IEEE, Microwave Theory and Techniques*, Vol 39, No 7, pp. 1239-1243, 1991.
- [30] M.K. Brewer, and A.V. Räsänen, *IEEE Trans. Microwave Theory and Techniques*, Vol. 30, pp. 708, 1982.
- [31] A.R Kerr, "An Adjustable Short-Circuit for Millimeter Waveguides," Electronics Division Internal Report No. 280, National Radio Astronomy Observatory, Charlottesville, VA 22903, July 1988.
- [32] A.R. Kerr, S.-K. Pan, M.J. Feldman, and A. Davidson, "Infinite Available Gain in a 115 GHz SIS Mixer," *Physica B*, vol. 108, pp 1369-1370, Sept. 1981.
- [33] S.-K. Pan, M.J. Feldman, A.R. Kerr, E.S. Palmer, J.A. Grange, and P. Timbie, "Superconducting Tunnel Junction Receiver for 2.6 mm," Digest of 8th International Conference on Infrared and Millimeter Waves, pp. M6.2/1-2, Dec. 1983.
- [34] D.P. Woody, R.E. Miller and M.J. Wengler, "85-115 GHz Receivers for Radio Astronomy," *IEEE trans. Microwaves Theory and Techniques*, Vol. MTT-33, 1985, pp. 90-95
- [35] R.Blundell, R.E. Miller, and K.H. Gundlach, "Understanding Noise in SIS Receivers," *Int. J. IR and MM Waves*, Vol 13, No. 1, pp. 3-26, 1992.
- [36] Q. Ke, and M.J. Feldman, "A Technique for Accurate Noise Temperature measurements for the Superconducting Quasiparticle Receiver," *Fourth international Symposium on Space Terahertz technology*, UCLA, 1993.
- [37] M.J. Feldman, "An Analytical Investigation of the Superconductor Quasiparticle Mixer in the Low Power Limit," *IEEE Trans. Magnetics*, Vol. 27, No. 2, pp. 2646-2649.